Impacts of PV Array Sizing on PV Inverter Lifetime and Reliability

Sangwongwanich, Ariya; Yang, Yongheng; Sera, Dezso; Blaabjerg, Frede

Published in:
Proceedings of 2017 IEEE Energy Conversion Congress and Exposition (ECCE)

DOI (link to publication from Publisher):
10.1109/ECCE.2017.8096675

Publication date:
2017

Document Version
Early version, also known as pre-print

Impacts of PV Array Sizing on PV Inverter Lifetime and Reliability

Ariya Sangwongwanich, Yongheng Yang, Dezso Sera, and Frede Blaabjerg
Department of Energy Technology, Aalborg University, Aalborg DK-9220, Denmark
ars@et.aau.dk, yoy@et.aau.dk, des@et.aau.dk, fbl@et.aau.dk

***Abstract*—In order to enable a more wide-scale utilization of PV systems, the cost of PV energy has to be comparable with other energy sources. Oversizing the PV array is one common approach to reduce the cost of PV energy, since it increases the PV energy yield during low solar irradiance conditions. However, oversizing the PV array will increase the loading of PV inverters, which may have undesired influence on the PV inverter lifetime and reliability. In that case, it may result in a negative impact on the overall PV energy cost, due to the increased maintenance for the PV inverters. This paper evaluates the lifetime of PV inverters considering the PV array sizing and installation sites, e.g., Denmark and Arizona. The results reveal that the PV array sizing has a considerable impact on the PV inverter lifetime and reliability, especially in Denmark, where the average solar irradiance level is relatively low.**

***Index Terms*—PV inverters, lifetime, reliability, mission profile, oversizing, Monte Carlo analysis.**

I. Introduction

With the aim to introduce more renewable energy and due to the still declining cost of PV panels and installation, the PV industry has had a high growth rate in the last decades [1]. Nevertheless, in order to further increase the PV penetration level, the cost of PV energy has to be reduced even further to make the PV power plant competitive with conventional power plants (e.g., fossil fuel based systems). It is recommended in [2] that the cost of PV energy (for the residential applications in US) has to be reduced from the current 0.18 USD/kWh to 0.05 USD/kWh by 2030. This is a challenging target to reduce the PV energy cost by more than 3 times in the near future. There are several ways to reduce the cost of PV energy and achieve the above target (e.g., improving efficiency, and enhancing components lifetime). Among others, one commonly (and practically) used solution is to oversize the PV arrays, where the rated power of the PV arrays is intentionally designed to be higher than the rated power of the PV inverter [3]–[5], as it is shown in Fig. 1. By doing so, the PV inverter will operate close to its rated power during a larger proportion of time, and more PV energy can be captured during the non-peak production period. As the PV panel cost is still declining, where the PV module price drops around 13% per year [6], oversizing the PV arrays becomes an attractive solution with a minor increase in the system cost, and thus reduce the total cost of PV energy [7]–[9].

The PV power extraction with oversized PV arrays is illustrated in Fig. 2, where the energy production of the PV system is increased due to the higher energy yield during the low solar irradiance condition. Nevertheless, oversizing the PV array might also have impact on the PV inverter operation, which is a link between the PV arrays and the grid. Impacts of oversizing the PV array on the cost of PV energy and design approaches to maximize the energy yield have been addressed in literature. In [10], the impact of PV array sizing on the energy cost is discussed for different system topologies. A similar study has been carried out in [11]–[13], where several installation sites (with different climate conditions) are considered. Optimum design solutions for oversizing the PV arrays have been proposed in [14]–[17] with the aim to maximize the PV energy yield while minimizing the system cost due to oversizing. Nevertheless, the prior-art work does not consider the impact of oversizing the PV arrays on the inverter lifetime and reliability. In other words, it is normally assumed that the PV inverter lifetime remains the same regardless of the PV array sizing. However, oversizing the PV array will inevitably affect the loading and thus the inverter lifetime and reliability. For instance, the PV inverter with oversized PV arrays will have higher power production and thereby higher thermal stresses on the critical components (e.g., power devices, and capacitors) than those without oversized PV arrays under the same mission profile (i.e., solar irradiance and temperature). This may result in a reduction in the component lifetime and

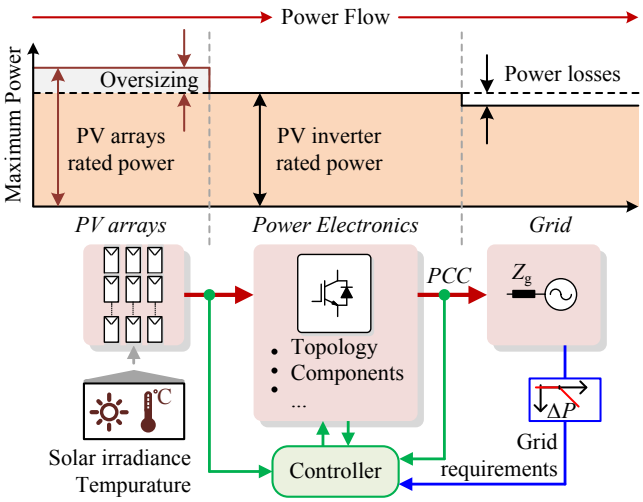

Fig. 1. Maximum power delivery at different power conversion stages of grid-connected PV system with oversized PV arrays.

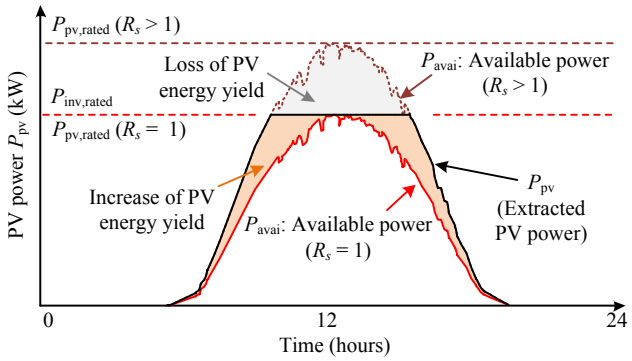

Fig. 2. PV power extraction with oversized PV arrays (P_{avai}: available PV power, P_{pv}: extracted PV power, $P_{pv,rated}$: PV array rated power, $P_{inv,rated}$: PV inverter rated power, $R_s = P_{pv,rated}/P_{inv,rated}$: sizing ratio).

the overall system reliability. As the cost associated with the PV inverter failure is around 59% of the total system cost, the PV inverter lifetime plays a crucial role in the cost assessment of the PV system [18]–[20]. In that case, the operational and maintenance cost of the PV inverter becomes significant, and may counteract benefits of the increased energy production, resulting in a negative impact on the overall PV energy cost. This issue has been pointed out in [8] and [13], but detailed lifetime analysis was not addressed.

To fill in this gap and address the above issue, this paper thus investigates the impacts of PV array sizing on the PV inverter lifetime and reliability. The lifetime evaluation is carried out with a case study of the installation sites in Denmark and Arizona, which is described in § II. The mission profile-based lifetime evaluation of the PV inverter is presented in § III, and it is applied to the case study in § IV. Then, the reliability assessment based on the Monte Carlo simulation is carried out in § V, where the parameter variation is introduced. The evaluation results show a significant increase in the thermal loading of the PV inverter in Denmark, especially during winter. In that case, the PV inverter lifetime is reduced significantly. Finally, concluding remarks are given in § VI.

II. Case Study Description

A. System Description

The system configuration and control structure of a single-phase grid-connected PV system are shown in Fig. 3. Here, a two-stage configuration is adopted, where two power converters - a boost dc-dc converter and a full-bridge dc-ac inverter (PV inverter) - are employed as an interface between the PV arrays and the grid [21]. This two-stage configuration is widely used in residential/commercial PV systems (e.g., with the rated power of 1 kW - 30 kW), where the power extraction from the PV arrays is controlled by the boost converter [22]. Normally, a Maximum Power Point Tracking (MPPT) algorithm is implemented in the boost converter by regulating the PV voltage v_{pv} at the Maximum Power Point (MPP) of the PV array in order to maximize the solar energy yield. However, in the case of oversized PV arrays, the extracted PV

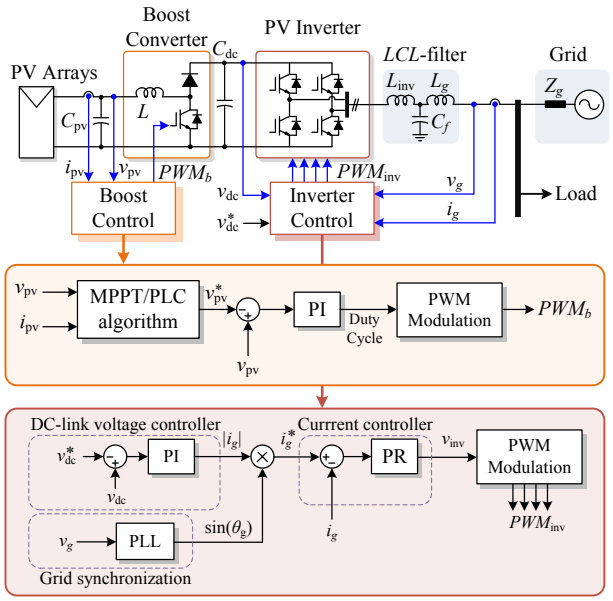

Fig. 3. System configuration and control structure of a two-stage single-phase grid-connected PV system (MPPT - Maximum Power Point Tracking, PLC - Power Limiting Control, PI - Proportional Integral, PR - Proportional Resonant, PLL - Phase-Locked Loop, PWM - Pulse Width Modulation).

power P_{pv} cannot exceed the PV inverter rated power $P_{inv,rated}$ due to safety reasons. In that case, the extracted PV power P_{pv} needs to be limited at the PV inverter rated power level (i.e., $P_{pv} = P_{inv,rated}$), which is achieved by regulating the PV power below the MPP [3]. At the grid-side, the PV inverter delivers the extracted power to the ac grid by regulating the dc-link voltage v_{dc} to be constant, which is achieved through the control of the grid current i_g using a current controller. Additionally, a Phase-Locked Loop (PLL) is also required for synchronization [23].

B. Operational Principle with Oversized PV Arrays

It is very common to define the sizing ratio R_s as the ratio of the PV array rated power at the Standard Test Condition (STC), $P_{pv,rated}$, over the PV inverter rated power $P_{inv,rated}$ (i.e., $R_s = P_{pv,rated}/P_{inv,rated}$). Usually, the PV system is designed to be oversized (i.e., $R_s > 1$) in order to capture more PV energy (e.g., during low solar irradiance condition) and increase the PV inverter utilization. However, due to the oversizing, the available PV power of the oversized PV arrays can be higher than the rated power of the PV inverter (e.g., during the peak power generation periods). In that case, the extracted PV power has to be curtailed at the rated inverter power level during the peak power generation periods (also called power limiting control, constant power generation control, and power clipping), which is achieved by moving the operating point of the PV array away from the MPP as shown in Fig. 4 [24]. Notably, this will inevitably result in loss of PV energy yield due to the power limitation, i.e., a negative impact on the levelized cost of solar energy. Thus, the sizing ratio has to be optimally designed by considering the system cost (e.g., PV

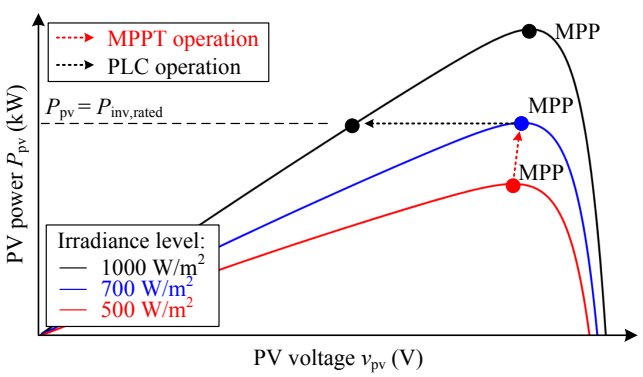

Fig. 4. Operational principle of PV system with oversized PV arrays with the Maximum Power Point Tracking (MPPT) and Power Limiting Control (PLC) operations (MPP: Maximum Power Point).

panels and inverters) and the solar resource (e.g., irradiance level) of the installation sites [14]–[17]. According to this, the sizing ratio varies with the installation sites, where the typical value (today) is in a range of $1 \leq R_s \leq 1.5$.

C. Mission Profile of the PV Systems

A mission profile is a representation of the operating condition of the system [25]. The solar irradiance and ambient temperature are considered as a mission profile of the PV systems, since the PV power production is strongly dependent on the two parameters. The one-year mission profiles recorded in Denmark and Arizona with a sampling rate of 5 minutes per sample are used in this study, as shown in Fig. 5. From the recorded mission profiles in Arizona, the average solar irradiance level is constantly high through the year. This is in contrast with the mission profile in Denmark, where the average solar irradiance level is relatively low through November to February. Additionally, the ambient temperature in Denmark also varies in a wide range with the minimum being around -18 °C during winter. The impact of oversizing the PV arrays on the PV inverter lifetime of the two installation sites will be different due to the mission profile characteristic, as it will be demonstrated later in this paper.

III. Mission Profile-based Lifetime Estimation

Lifetime of PV inverters can be considerably influenced by the operating condition of the system, referred to as mission profiles (i.e., solar irradiance and ambient temperature) [26]. For instance, the PV power production is mainly determined by the solar irradiance and ambient temperature conditions of the system, and it will eventually be translated into the thermal stress of the PV inverter. For some critical components in the PV inverter (e.g., power devices), this thermal stress can cause failure after a given number of thermal cycles, e.g., resulting in a bond wire lift-off of power device [25]. Therefore, the mission profile is normally taken into consideration in the lifetime evaluation process, in which three main tasks are involved [25], [27]–[29]: 1) Mission profile translation to

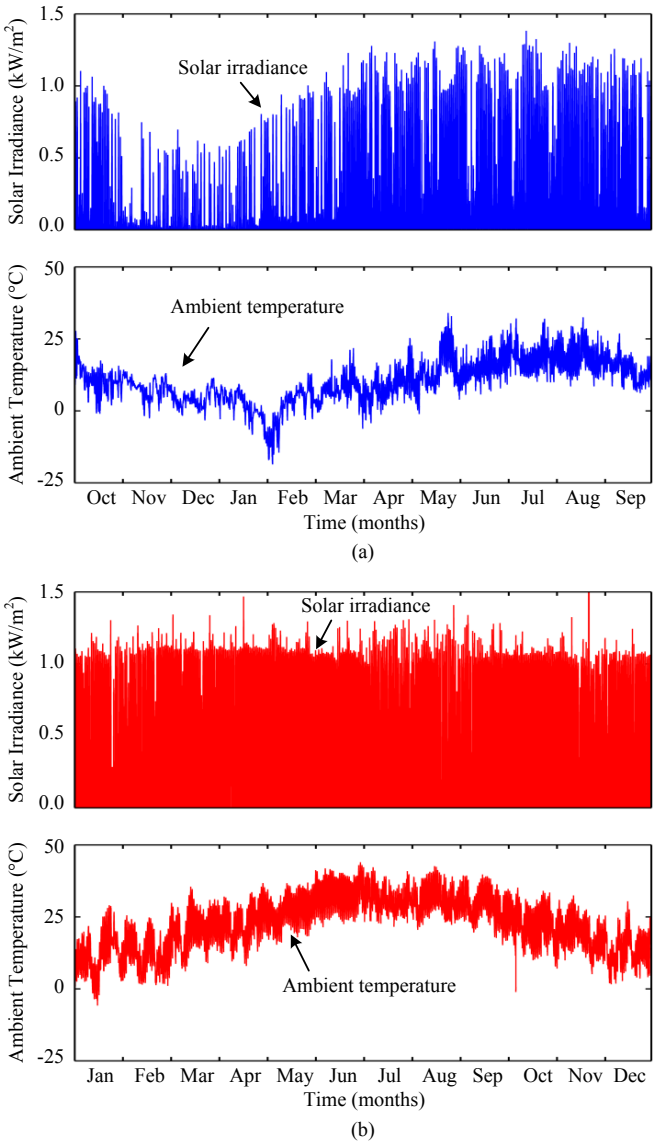

Fig. 5. Yearly mission profiles (i.e., irradiance and ambient temperature with a sampling rate of 5 mins per sample) at: (a) Denmark and (b) Arizona.

thermal loading, 2) Thermal cycling interpretation, 3) Lifetime modeling of power devices. The flow diagram of this procedure is summarized in Fig. 6, and will be elaborated in the following.

A. Mission Profile Translation to Thermal Loading

As the first step, the mission profile needs to be translated into the thermal loading of the power device, which is one of the main life-limiting components of the PV inverter. For a given solar irradiance and ambient temperature profiles, the PV power at the MPP of the PV array P_{mpp} can be determined by using the PV panel characteristic model [31]. In this case, the PV panel model with the same rated power as the PV inverter is considered (representing the case with non-oversized PV arrays). Then, the available PV power P_{avai}

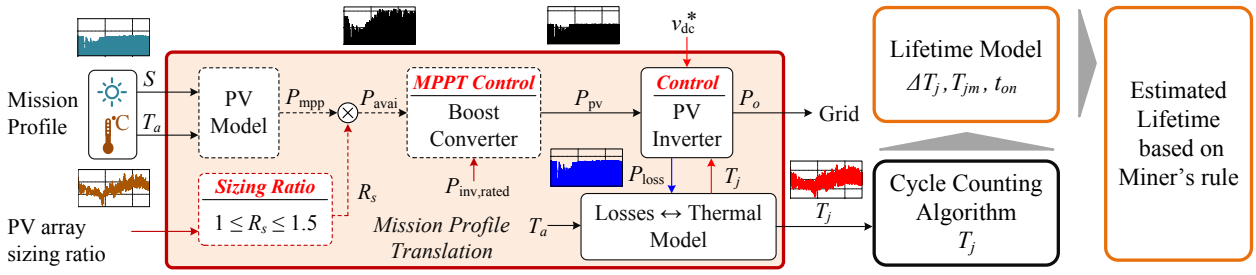

Fig. 6. Mission profile-translation diagram of a single-phase PV system, where the PV array sizing ratio R_s is taken into account [30].

can be calculated by multiplying the PV power at the MPP P_{mpp} with the sizing ratio of the PV system R_s. This implies that the actual available PV power can be higher than the PV inverter rated power for the case with oversized PV arrays (i.e., $R_s > 1$). Afterwards, the extracted PV power P_{pv} (i.e., input power of the PV inverter) is determined by taking the MPPT operation efficiency (99%) and the power limiting operation (when $P_{\text{avai}} > P_{\text{inv,rated}}$) into account. In other words, the maximum extracted PV power is limited to the PV inverter rated power. Then, considering the PV inverter efficiency, the power losses dissipated in the power devices, P_{loss}, can be obtained and applied to the thermal model of the power device. By doing so, the junction temperature profile of the power device T_j during operation is obtained. Normally, a Look-Up Table (LUT) generated from the conduction and switching losses of the power device and the thermal impedance given in the datasheet is employed to assist a long-term simulation (e.g., one-year mission profiles) [30].

B. Thermal Cycling Interpretation

From the previous step, thermal loading of the power device in the PV inverter for a given mission profile can be obtained. However, the obtained junction temperature profile usually contains the mission profile dynamics. In order to apply such an irregular junction temperature profile to the lifetime model, which is based on the empirical data, a cycle counting algorithm is needed for thermal cycling interpretation [28]. This method has been widely used in the lifetime and stress analysis related to the thermal cycling. For instance, a rainflow counting algorithm can be employed for dividing the irregular profile into several regular cycles according to the cycle amplitude, its average value, and the cycle period. By applying this method to the device junction temperature profile, the number of cycles n_i at a certain cycle amplitude ΔT_j, mean junction temperature T_{jm}, and cycle period t_{on} can be obtained (see Fig. 6). The information can be directly applied to the lifetime model and the lifetime of the power device can then be evaluated.

C. Lifetime Model of the Power Devices

According to field experiences, there are several components (e.g., power devices, capacitors, gate drivers, fans and etc.) that can cause failures in the PV inverters [19]. In fact, the failure mechanism of each components may have a cross-effect on the reliability of other components in the system, leading to a very complicated analysis. In this paper, only the failure mechanism related to the thermal cycling of the power device is considered as an example for simplicity. The lifetime model of the power device (e.g., IGBT) subjected to the thermal cycling is given as

$$N_f = A \times (\Delta T_j)^{\alpha} \times (ar)^{\beta_1 \Delta T_j + \beta_0} \times \left[\frac{C+(t_{on})^{\gamma}}{C+1}\right] \times \exp\left(\frac{E_a}{k_b \times T_{jm}}\right) \times f_d \quad (1)$$

where N_f is the number of cycles to failure [32]. The mean junction temperature T_{jm}, cycle amplitude ΔT_j, and cycle period t_{on} are the stress level obtained from the cycle counting algorithm, while the other parameters are given in Table I.

TABLE I
PARAMETERS OF THE LIFETIME MODEL OF AN IGBT MODULE [32].

Parameter	Value	Experimental condition
A	3.4368×10^{14}	
α	-4.923	$64\ \text{K} \le \Delta T_j \le 113\ \text{K}$
β_1	-9.012×10^{-3}	
β_0	1.942	$0.19 \le ar \le 0.42$
C	1.434	
γ	-1.208	$0.07\ \text{s} \le t_{on} \le 63\ \text{s}$
f_d	0.6204	
E_a	0.06606 eV	$32.5\ ^\circ\text{C} \le T_j \le 122\ ^\circ\text{C}$
k_B	8.6173324×10^{-5} eV/K	

By using the Miner's rule [28], the Life Consumption (LC) or damage of the power device, can be calculated as [28]

$$LC = \sum_i \frac{n_i}{N_{fi}} \quad (2)$$

where n_i is the number of cycles (obtained from the rainflow analysis) for a certain T_{jm}, ΔT_j, and t_{on}, and N_{fi} is the number of cycles to failure calculated from (1) at that specific stress condition. The LC is an indicator of how much lifetime of the power device is consumed (or damaged) during the operation (e.g., according to the applied mission profile) [25]. For example, the LC calculated from a one-year mission profile will represent a yearly LC of the power device. When the LC is accumulated to unity (e.g., after several years of

TABLE II
PARAMETERS OF THE TWO-STAGE SINGLE-PHASE PV SYSTEM (FIG. 3).

PV array rated power	6 kW (with sizing ratio R_s = 1)
PV inverter rated power	6 kW
Boost converter inductor	L = 1.8 mH
DC-link capacitor	C_{dc} = 1000 μF
LCL-filter	L_{inv} = 4.8 mH, L_{g} = 2 mH, C_f = 4.3 μF
Switching frequency	Boost converter: f_b = 16 kHz, Full-Bridge inverter: f_{inv} = 8 kHz
DC-link voltage	v_{dc}^* = 450 V
Grid nominal voltage (RMS)	V_g = 230 V
Grid nominal frequency	ω_0 = 2π×50 rad/s

operation), the power device is considered to reach its end of life, and the lifetime of the PV inverter can be predicted.

IV. LIFETIME EVALUATION (CASE STUDY)

In this section, the lifetime evaluation discussed in § III is applied to the two-stage PV system in Fig. 3 with the parameters shown in Table II. The case study is based on the mission profiles in Denmark and Arizona (Fig. 5) with different sizing ratios. The thermal loading of the power device and the corresponding LC are evaluated.

A. Thermal Loading of PV Inverters

The mean junction temperature T_{jm} and the cycle amplitude ΔT_j of the PV inverter installed in Denmark and Arizona are shown in Figs. 7 and 8, respectively. An example of two different cases with $R_s = 1$ (i.e., non-oversized PV arrays) and $R_s = 1.4$ (i.e., oversized PV arrays) are considered. It can be seen from Fig. 7 that the PV inverter installed in Denmark with oversized PV arrays (i.e., $R_s = 1.4$) has a strong increase in the thermal loading compared to the case where $R_s = 1$ (i.e., mean junction temperature and cycle amplitude), especially during November through February (when the solar irradiance level is low). The impact of oversizing PV arrays is less pronounced with the PV system in Arizona, where only a small increase in the thermal loading of the PV inverter is observed in Fig. 8. This is due to the fact that the PV inverter installed in Arizona with $R_s = 1.4$ mostly operates in the power limiting mode (i.e., $P_{\text{pv}} = P_{\text{inv,rated}}$) because of the high average solar irradiance level through the year. In that case, oversizing the PV array will not significantly increase the PV power production and thus the thermal loading of the PV inverter.

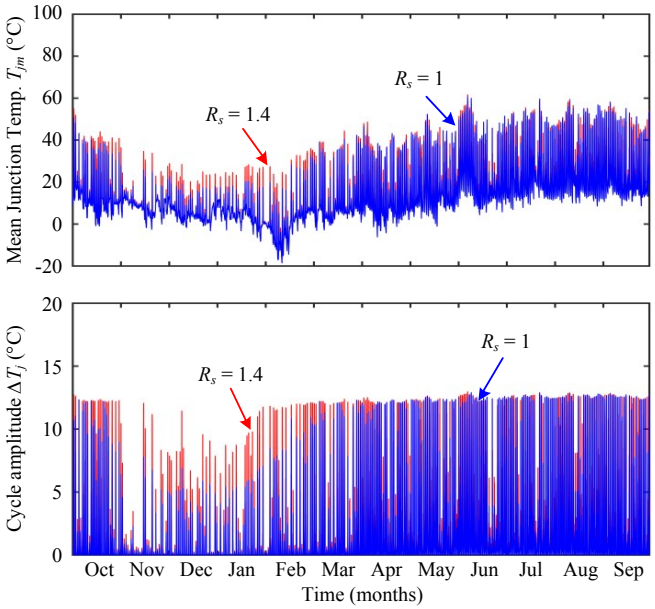

Fig. 7. Mean junction temperature T_{jm} and cycle amplitude ΔT_j of the power device under a mission profile in Denmark with different sizing ratios (blue plot: $R_s = 1$, red plot: $R_s = 1.4$).

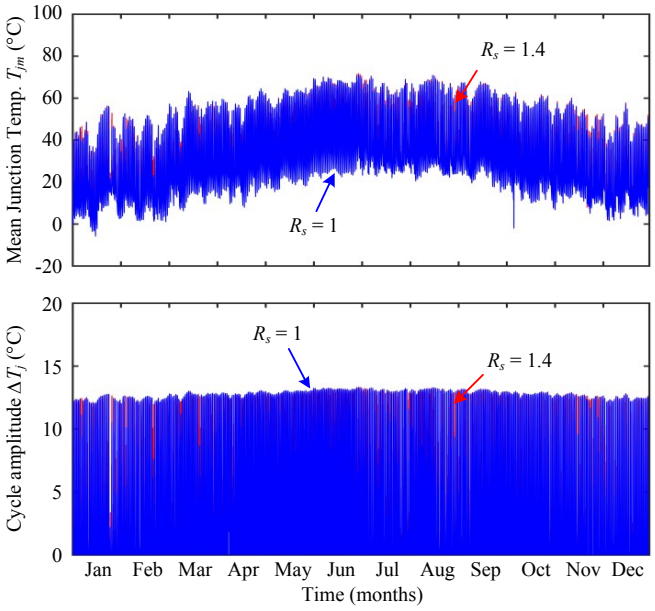

Fig. 8. Mean junction temperature T_{jm} and cycle amplitude ΔT_j of the power device under a mission profile in Arizona with different sizing ratios (blue plot: $R_s = 1$, red plot: $R_s = 1.4$).

B. Lifetime Evaluation

From the thermal loading of the PV inverter (i.e., mean junction temperature and cycle amplitude) in Figs. 7 and 8, the corresponding LC of the PV inverter during one-year operation can be calculated following (2). The normalized LC (compared with the case without oversizing) of the PV system with different sizing ratios (e.g., $1 \leq R_s \leq 2$) is shown in Fig. 9. As it is expected, the impact of oversizing on the LC is significant with the Denmark mission profile, where the LC increases considerably as R_s increases (see Fig. 9(a)). Notably, the higher LC results in shorter lifetime of the PV inverter. In contrast, the LC of the PV inverter installed in Arizona is less affected by the sizing ratio of the PV arrays (see Fig. 9(b)). In this case, the LC only increases slightly, and it saturates around 1.5 times of the initial LC (i.e., LC without oversizing). Again, this is simply due to the mission profile characteristic (especially the solar irradiance profile) in

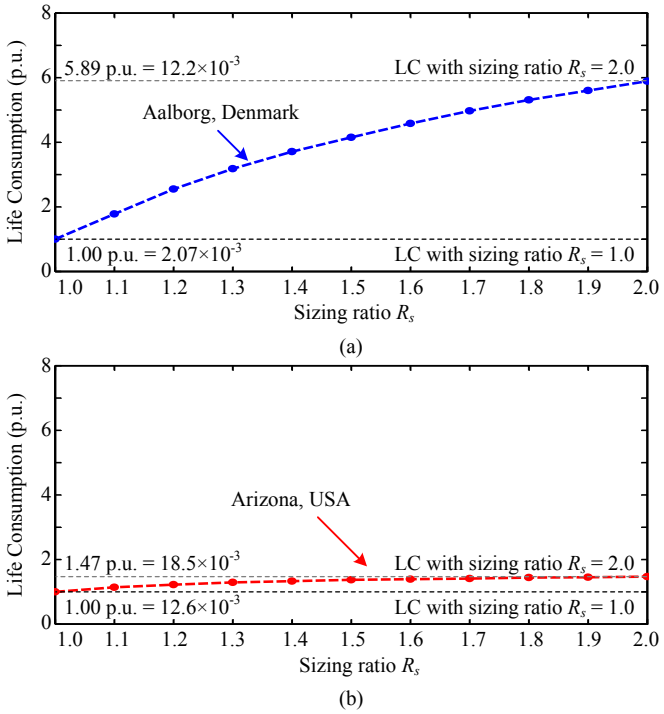

Fig. 9. Normalized life consumption of the power device in PV inverter with different sizing ratios for the mission profile in: (a) Denmark and (b) Arizona.

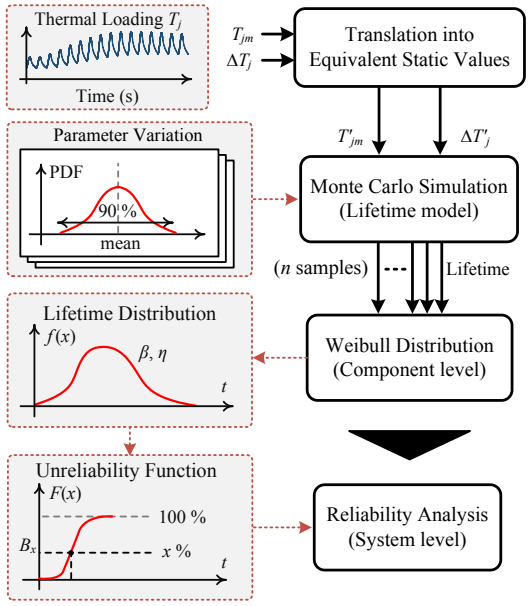

Fig. 10. Flow diagram of the Monte Carlo-based reliability assessment of PV inverter [35].

Denmark, where the average irradiance level is relatively low during the winter. By oversizing the PV arrays, the PV power production during the winter is increased considerably without reaching the rated PV inverter power limit. On the other hand, the solar irradiance in Arizona is relatively high throughout the year. Thus, oversizing the PV arrays can easily lead to a power limiting operation, due to the maximum capability of the PV inverter. Therefore, only a small increase in the PV power production is obtained, and thus the impact on the LC of the PV inverter is less significant compared to that in Denmark.

V. Reliability Analysis

From the previous lifetime evaluation, the LC during one-year operation can be calculated from the mission profile. In order to evaluate the reliability of the system, parameter variations need to be introduced in the lifetime evaluation process (e.g., lifetime model and the stress parameters) by using the Monte Carlo simulation [33]–[35]. By doing so, the lifetime distribution and the unreliability function of the power device can be expressed in terms of statistical value, and the reliability metrics such as B_x lifetime can be obtained [36].

A. Monte Carlo Simulation

The overall process of the Monte Carlo-based reliability assessment is shown in Fig. 10. The basic idea of this method is to model the parameter used in the calculation (e.g., lifetime model and stress parameters) with a certain distribution function, instead of using a fixed parameter. In this way, the parameter variation can be introduced during the calculation. Then, the lifetime evaluation (following the approach in § III) is carried out with a population of n samples. By doing so, the lifetime distribution (e.g., the Weibull distribution) of the power device $f(x)$ can be constructed from the lifetime yield of n different samples. Based on this result, it is also possible to obtain the unreliability function of the power device $F(x)$, which is a cumulative function of the lifetime distribution [36]. The unreliability function can be used to indicate the development of failure overtime. For instance, the time when $x\%$ of population have failed can be obtained from the unreliability function, and it is normally referred to as B_x lifetime. Notably, for the system with several components (e.g., the PV inverter with several power devices), the reliability block diagram, which represents the reliability interaction among components in the system, is required for calculating the reliability of the entire system. A step-by-step system-level reliability evaluation process has been discussed in details in [33]–[35].

B. Reliability Assessment (Case Study)

The reliability assessment of the PV inverter is carried out under two mission profiles: Denmark and Arizona. The unreliability function of the PV inverter is calculated from the sample of 10000 population (e.g., n = 10000) where the parameter variation of 5% is introduced. The unreliability function of the PV inverter $F(x)$ with different sizing ratio R_s is shown in Fig. 11. It can be noticed from the unreliability function $F(x)$ in Fig. 11(a) that the failure rate of the PV inverter in Denmark increases relatively fast with the increased sizing ratio. On the other hand, only a small change in the unreliability curve with different sizing ratios is observed

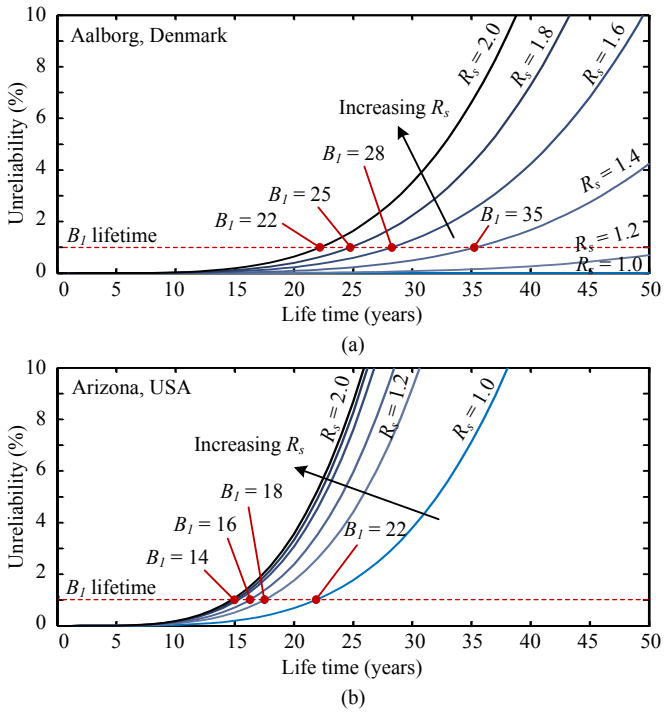

Fig. 11. Unreliability function of the PV inverter with different sizing ratios for the mission profile in: (a) Denmark and (b) Arizona.

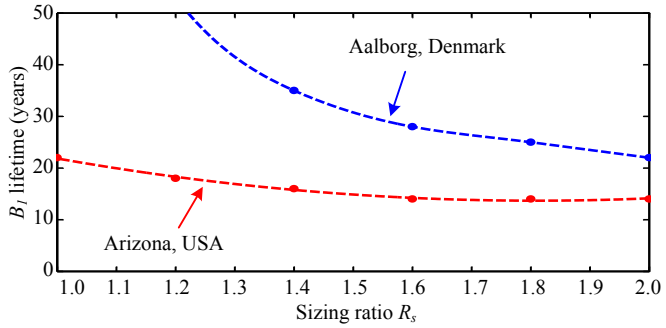

Fig. 12. B_1 lifetime of the PV inverter with different sizing ratios for the mission profile in Denmark and Arizona.

under the Arizona mission profile in Fig. 11(b), especially when the sizing ratio is higher than 1.4 (i.e., $R_s \geq 1.4$).

From the unreliability function in Fig. 11, the B_1 lifetime of the PV inverter with different sizing ratios can be obtained by considering the time when 1% of the population have failed, as it is also indicated in the same figure, and used as a reliability metric. Notably, the B_1 lifetime of the PV inverter with the Denmark mission profile is higher than 50 years for the sizing ratio below 1.2 (i.e., $R_s \leq 1.2$), which is not practical (in general). In that case, other failure mechanisms or components will be dominant during this time period, and the B_1 lifetime obtained from the thermal cycling related failure mechanism may not represent the main life-limiting factor of the PV inverter.

The B_1 lifetime of the PV inverter with different sizing ratios for the two mission profiles is summarized in Fig. 12, where it can be seen that the B_1 lifetime of the PV inverter in Denmark decreases considerably as the sizing ratio R_s increases. In contrast, the impact of the sizing ratio R_s is less significant in the case of Arizona mission profile. For example, only a small reduction in the PV inverter lifetime is observed (i.e., around 27%) when the sizing ratio of the PV system is increased from R_s = 1 to R_s = 1.4. When the sizing ratio is further increased from R_s = 1.4 to R_s = 2, the B_1 lifetime of the PV inverter remains almost constant at B_1 = 14 years (e.g., the lifetime difference is less than a year). The above reliability assessment results are in agreement with the previous lifetime evaluation in § IV, where the impact of sizing ratio is less pronounced in the case of the Arizona mission profile due to the power limiting operation of the PV inverter.

VI. Conclusion

The impact of the PV array sizing on the PV inverter lifetime and reliability has been investigated in this paper. The mission profile-based lifetime evaluation has been carried out on PV systems installed in Denmark and Arizona with different sizing ratios. Moreover, the Monte Carlo simulation was employed for the reliability assessment, where parameter variations are taken into consideration. The evaluation results show a considerable impact of the PV array sizing on the lifetime of the PV inverter installed in Denmark, where the PV inverter thermal loading increases considerably with the oversized PV arrays. In contrast, the PV inverter installed in Arizona has less impacts from the PV array oversizing, due to the average high irradiance condition. In that case, the increased loading due to the oversizing is less significant because of the power limitation of the PV inverter.

Acknowledgment

This work was supported in part by the European Commission within the European Union's Seventh Framework Program (FP7/2007-2013) through the SOLAR-ERA.NET Transnational Project (PV2.3 - PV2GRID), by Energinet.dk (ForskEL, Denmark, Project No. 2015-1-12359), and in part by the Research Promotion Foundation (RPF, Cyprus, Project No. KOINA/SOLAR-ERA.NET/0114/02).

References

[1] REN21, "Renewables 2017: Global Status Report (GRS)," 2017. [Online]. Available: http://www.ren21.net/.

[2] National Renewable Energy Laboratory, "On the path to sunshot: The role of advancements in solar photovoltaic efficiency, reliability, and costs," Tech. Rep. No. NREL/TP-6A20-65872, 2016.

[3] J. Fiorelli and M. Zuercher-Martinson, "How oversizing your array-to-inverter ratio can improve solar-power system performance," *Solar Power World*, vol. 7, pp. 42–48, 2013.

[4] T. Khatib, A. Mohamed, and K. Sopian, "A review of photovoltaic systems size optimization techniques," *Renew. Sustain. Energy Rev.*, vol. 22, pp. 454–465, 2013.

[5] M. Hussin, A. Omar, S. Shaari, and N. M. Sin, "Review of state-of-the-art: Inverter-to-array power ratio for thin-film sizing technique," *Renewable and Sustainable Energy Reviews*, vol. 74, pp. 265–277, 2017.

[6] Fraunhofer ISE, "Recent Facts about Photovoltaics in Germany," January 9, 2017. [Online]. Available: http://www.pv-fakten.de/.

[7] SMA, "7 reasons why you should oversize your PV array," Dec. 2015. [Online]. Available: http://en.sma-sunny.com/en/7-reasons-why-you-should-oversize-your-pv-array-2/

[8] Global Sustainable Energy Solutions (GSES) India, "Oversizing PV arrays," Tech. Rep., 2014.

[9] SolarEdge, "Oversizing of SolarEdge inverters, technical note," Tech. Rep., July 2016.

[10] F. He, Z. Zhao, and L. Yuan, "Impact of inverter configuration on energy cost of grid-connected photovoltaic systems," *Renewable Energy*, vol. 41, pp. 328–335, 2012.

[11] B. Burger and R. Ruther, "Site-dependent system performance and optimal inverter sizing of grid-connected PV systems," in *Proc. of PVSEC*, pp. 1675–1678, Jan. 2005.

[12] B. Burger and R. Ruther, "Inverter sizing of grid-connected photovoltaic systems in the light of local solar resource distribution characteristics and temperature," *Solar Energy*, vol. 80, no. 1, pp. 32–45, 2006.

[13] J. Good and J. X. Johnson, "Impact of inverter loading ratio on solar photovoltaic system performance," *Applied Energy*, vol. 177, pp. 475–486, Sep. 2016.

[14] J. D. Mondol, Y. G. Yohanis, and B. Norton, "Optimal sizing of array and inverter for grid-connected photovoltaic systems," *Solar Energy*, vol. 80, no. 12, pp. 1517–1539, Dec. 2006.

[15] S. Chen, P. Li, D. Brady, and B. Lehman, "Determining the optimum grid-connected photovoltaic inverter size," *Solar Energy*, vol. 87, pp. 96–116, 2013.

[16] R. Mounetou, I. B. Alcantara, A. Incalza, J. Justiniano, P. Loiseau, G. Piguet, and A. Sabene, "Oversizing array-to-inverter (dc-ac) ratio: What are the criteria and how to define the optimum?" in *Proc. Eur. Photovolt. Sol. Energy Conf. Exhib.*, pp. 2813–2821, Sep. 2014.

[17] R. S. Faranda, H. Hafezi, S. Leva, M. Mussetta, and E. Ogliari, "The optimum PV plant for a given solar dc/ac converter," *Energies*, vol. 8, no. 6, pp. 4853–4870, May 2015.

[18] L. M. Moore and H. N. Post, "Five years of operating experience at a large, utility-scale photovoltaic generating plant," *Progress Photovoltaics: Res. Appl.*, vol. 16, no. 3, pp. 249–259, 2008.

[19] A. Golnas, "PV system reliability: An operator's perspective," *IEEE J. of Photovolt.*, vol. 3, no. 1, pp. 416–421, Jan. 2013.

[20] F. Baumgartner, O. Maier, D. Schar, D. Sanchez, and P. Toggweiler, "Survey of operation and maintenance costs of PV plants in Switzerland," in *Proc. Eur. Photovolt. Sol. Energy Conf. Exhib.*, pp. 1583–1586, Sep. 2015.

[21] S.B. Kjaer, J.K. Pedersen, and F. Blaabjerg, "A review of single-phase grid-connected inverters for photovoltaic modules," *IEEE Trans. Ind. Appl.*, vol. 41, no. 5, pp. 1292–1306, Sep. 2005.

[22] Y. Yang and F. Blaabjerg, "Overview of single-phase grid-connected photovoltaic systems," *Electric Power Components and Sys.*, vol. 43, no. 12, pp. 1352–1363, 2015.

[23] F. Blaabjerg, R. Teodorescu, M. Liserre, and A.V. Timbus, "Overview of control and grid synchronization for distributed power generation systems," *IEEE Trans. Ind. Electron.*, vol. 53, no. 5, pp. 1398–1409, Oct. 2006.

[24] A. Sangwongwanich, Y. Yang, and F. Blaabjerg, "High-performance constant power generation in grid-connected PV systems," *IEEE Trans. Power Electron.*, vol. 31, no. 3, pp. 1822–1825, Mar. 2016.

[25] M. Musallam, C. Yin, C. Bailey, and M. Johnson, "Mission profile-based reliability design and real-time life consumption estimation in power electronics," *IEEE Trans. Power Electron.*, vol. 30, no. 5, pp. 2601–2613, May 2015.

[26] C. Felgemacher, S. Araujo, C. Noeding, P. Zacharias, A. Ehrlich, and M. Schidleja, "Evaluation of cycling stress imposed on IGBT modules in PV central inverters in sunbelt regions," in *Proc. of CIPS*, pp. 1–6, Mar. 2016.

[27] H. Wang, M. Liserre, and F. Blaabjerg, "Toward reliable power electronics: Challenges, design tools, and opportunities," *IEEE Ind. Electron. Mag.*, vol. 7, no. 2, pp. 17–26, Jun. 2013.

[28] H. Huang and P. A. Mawby, "A lifetime estimation technique for voltage source inverters," *IEEE Trans. Power Electron.*, vol. 28, no. 8, pp. 4113–4119, Aug. 2013.

[29] Y. Yang, A. Sangwongwanich, and F. Blaabjerg, "Design for reliability of power electronics for grid-connected photovoltaic systems," *CPSS Trans. Power Electron. Appl.*, vol. 1, no. 1, pp. 92–103, 2016.

[30] Y. Yang, H. Wang, F. Blaabjerg, and K. Ma, "Mission profile based multi-disciplinary analysis of power modules in single-phase transformerless photovoltaic inverters," in *Proc. of EPE*, pp. 1–10, Sep. 2013.

[31] D. Sera, R. Teodorescu, and P. Rodriguez, "PV panel model based on datasheet values," in *Proc. of ISIE*, pp. 2392–2396, Jun. 2007.

[32] U. Scheuermann, R. Schmidt, and P. Newman, "Power cycling testing with different load pulse durations," in *Proc. of PEMD 2014*, pp. 1–6, Apr. 2014.

[33] P. D. Reigosa, H. Wang, Y. Yang, and F. Blaabjerg, "Prediction of bond wire fatigue of IGBTs in a PV inverter under a long-term operation," *IEEE Trans. Power Electron.*, vol. 31, no. 10, pp. 7171–7182, Oct. 2016.

[34] K. Ma, H. Wang, and F. Blaabjerg, "New approaches to reliability assessment: Using physics-of-failure for prediction and design in power electronics systems," *IEEE Power Electron. Mag.*, vol. 3, no. 4, pp. 28–41, Dec. 2016.

[35] A. Sangwongwanich, Y. Yang, D. Sera, and F. Blaabjerg, "Lifetime evaluation of grid-connected PV inverters considering panel degradation rates and installation sites," *IEEE Trans. Power Electron.*, vol. PP, no. 99, pp. 1–1, 2017.

[36] H. S.-H. Chung, H. Wang, F. Blaabjerg, and M. Pecht, *Reliability of Power Electronic Converter Systems*. IET, 2015.